Vietnam Journal of Earth Sciences, 47(2), 252–271, https://doi.org/10.15625/2615-9783/22704

Vietnam Journal of Earth Sciences
https://vjs.ac.vn/index.php/jse

Monitoring spatial-temporal dynamics of drought over Yok Don National Park using Temperature-soil Moisture Dryness Index (TMDI)

Mai Son Le[1], Manh Hung Nguyen[2,3], Duy Toan Dao[4*], Duc-Tu Dinh[5], Thai Binh Tran[2], Thi Kim Dung Le[6]

[1]*Space Technology Institute, Vietnam Academy of Science and Technology, Hanoi, Vietnam*
[2]*Vietnam National Space Center, Vietnam Academy of Science and Technology, Hanoi, Vietnam*
[3]*Graduate University of Science and Technology, Vietnam Academy of Science and Technology, Hanoi, Vietnam*
[4]*Department of Geodesy & Geomatics Engineering, Faculty of Bridge and Road, Hanoi University of Civil Engineering, Hanoi, Vietnam*
[5]*Ninh Binh Hydro-Meteorological Center, Northern Delta and Midland Regional Hydro-Meteorological Center, Ninh Binh province, Vietnam*
[6]*Faculty of Land Administration, Hanoi University of Natural Resources and Environment, Hanoi, Vietnam*

Received 11 January 2025; Received in revised form 25 March 2025; Accepted 15 April 2025

ABSTRACT

This study investigates the spatio-temporal patterns of drought and their teleconnection with land surface properties in Yok Don National Park during the dry season using the Temperature-Soil Moisture Dryness Index (TMDI). This index is derived from the relationship between the Normalized Difference Land Heat Index and Land Surface Temperature, extracted from Landsat-8 data acquired in the mid-dry season from 2014 to 2023. Results reveal increasing drought severity starting in 2014, peaking during 2015–2016, and decreasing from 2017 to 2020. Drought conditions escalated again during 2021–2022 before moderating by 2023. These trends align with in-situ precipitation data recorded at a nearby meteorological station, highlighting varied impacts on forest types. Areas covered by deciduous broadleaf forests experienced pronounced drought effects, whereas evergreen broadleaf forests showed greater resilience. Land surface evapotranspiration rates obtained from NASA's MOD16A2GF dataset were used to evaluate TMDI performance. During the dry seasons from 2014 to 2023, TMDI exhibited a consistent negative correlation with evapotranspiration, with coefficients ranging from -0.55 to -0.70. This demonstrates TMDI's effectiveness in capturing land surface water availability and assessing drought conditions. The findings provide crucial insights into drought monitoring and management for Yok Don National Park and other water-scarce regions, reinforcing TMDI's value in sustainable forest management and drought mitigation.

Keywords: Drought Monitoring, Yok Don National Park (Vietnam), Temperature-Soil Moisture Dryness Index (TMDI), Landsat-8 images.

1. Introduction

Drought is a prolonged period of deficient rainfall, leading to dryness and affecting water resources, agricultural production, and human livelihoods. Based on its impacts, drought is classified into four major types:

*Corresponding author, Email: toandd@huce.edu.vn

meteorological drought, agrarian drought, hydrological drought, and socio-economic drought (Wilhite and Glantz, 1985). Drought ranks among the most costly and destructive natural disasters, simultaneously affecting various sectors and communities. It contributes to soil deterioration, water shortages, crop failures, wildfires, and other disasters. Drought significantly impacts ecological and socio-economic systems (Zhong et al., 2019). Combined with extreme heat, droughts are responsible for a 9%–10% reduction in global cereal production (Lesk et al., 2016). In the Netherlands, drought severely affected multiple sectors, causing damages estimated between 450 and 2,080 million Euros (EUR) during the summer of 2018 (Philip et al., 2020). In China, annual agricultural drought losses can reach up to 16,302 million tons, accounting for over 60% of all grain losses caused by natural disasters from 1950 to 2016 (Zhang et al., 2019; Cai et al., 2023). Vietnam is identified as particularly vulnerable to droughts in Southeast Asia, with El Niño events driving moderate to severe impacts (MONRE, 2019; UNESCAP, 2019; WorldBank, 2021). Droughts' increasing severity and duration have profoundly affected Vietnam's agricultural sector, which employs over half of the population and contributes roughly 20% to the nation's GDP (Le et al., 2021). In early 2016, a severe drought caused significant economic damage across 18 provinces, with estimated losses reaching approximately US$674 million, equivalent to 0.35% of the country’s 2015 GDP. The drought also left about 2 million people facing acute water shortages, requiring urgent humanitarian aid (UNDP, 2016). Globally, nearly one-third of the population resides in water-scarce regions, and an estimated 1.1 billion people do not have reliable access to safe drinking water. Drought affects about 7.5% of Earth's land area, and its impact is worsening, with the proportion of land experiencing severe drought doubling from the 1970s to the early 2000s (Belal et al., 2014). Therefore, monitoring drought conditions is essential for providing crucial information that aids in predicting and mitigating its impacts. It also supports decision-making in water resource management, builds resilience against climate change, and protects vulnerable communities and ecosystems.

A meteorological drought is a significant deficiency in precipitation over a specific period and region. Traditionally, drought indices determined from in-situ rainfall data recorded at meteorological stations over long periods are used to identify drought situations (Shahabfar and Eitzinger, 2013; Asefjah et al., 2014). However, traditional drought monitoring methods often suffer from data density and spatial coverage limitations, focusing on localized areas rather than offering a complete view of extensive regions. This dependence on site-specific data makes it challenging to accurately assess drought conditions over large geographic areas, reducing the effectiveness of monitoring strategies (Mishra et al., 2015). As a result, traditional approaches may not fully capture the overall scope or severity of drought events (Fung et al., 2020).

Technological advancements have revolutionized drought monitoring, offering precise, timely, and comprehensive data through satellite-based remote sensing, hydrological and climate models, GIS, spatial analysis, and machine learning. Remote sensing stands out due to its extensive coverage, continuous data collection, objectivity, and promptness, making it a

leading tool for addressing the limitations of traditional in-situ methods. It quickly captures detailed spectral data on land surface features such as soil moisture, evapotranspiration rates, vegetation health, and surface temperatures (Maes and Steppe, 2012). These parameters are vital for assessing drought severity and progression, leading to a more comprehensive understanding of drought dynamics and better-informed decision-making (Belal et al., 2014). By integrating various datasets, remote sensing provides a complete view of the factors influencing drought conditions. This capability has facilitated the development of numerous models and indices for effectively monitoring and forecasting droughts across different spatial scales (Vicente-Serrano et al., 2015). Remote sensing-based indices for drought monitoring can be categorized into single and combined indices. Single indices typically focus on aspects of drought, such as vegetation health, soil moisture, water availability, and land surface temperature. These are widely utilized due to their simplicity and effectiveness. In contrast, combined indices integrate multiple variables to offer a more comprehensive approach to capturing drought dynamics. Examples include the Normalized Difference Vegetation Index (NDVI), Enhanced Vegetation Index (EVI), Vegetation Condition Index (VCI), and Land Surface Temperature (LST) (Cai et al., 2023; Mullapudi et al., 2023). Other indices, such as the Normalized Difference Moisture Index (NDMI) (Das et al., 2023), the Normalized Drought Dryness Index (NDDI) (Gu et al., 2007), Modified Normalized Drought Dryness Index (MNDDI) (Nguyen et al., 2024), and Temperature Vegetation Dryness Index (TVDI) (Sandholt et al., 2002), were developed to enhance accuracy and applicability in different contexts. Among these, NDVI is particularly well-known for its effectiveness in evaluating vegetation health. It is widely used to determine whether plants are experiencing water stress or drought conditions. NDVI can function independently or be integrated into broader frameworks for drought assessment, making it a key indicator for tracking vegetation health and understanding drought patterns. However, NDVI's sensitivity to early signs of water stress may be limited, as it responds slowly when plant leaves remain green despite water shortages. Thus, while NDVI provides valuable insights into drought conditions, its effectiveness can vary based on the specific landscape characteristics being analyzed (Van Hoek et al., 2016). Additionally, factors such as plant diversity, soil types, and varying environmental conditions can affect how well NDVI captures the impact of drought.

In 2019, the Normalized Difference Latent Heat Index (NDLI) was introduced and proven to be an effective new method for evaluating surface water availability (Liou et al., 2019). This index utilizes spectral reflectance data from the green, red, and shortwave infrared (SWIR 1) channels, offering valuable insights into surface water presence and moisture distribution across different land covers. Recognizing the role of temperature in drought analysis, the Temperature-Soil Moisture Dryness Index (TMDI) was developed by examining scatter plots of LST and NDLI values (Le and Liou, 2022). The TMDI integrates LST and NDLI data to assess surface water shortages thoroughly, enhancing drought prediction and severity evaluation. Derived solely from remote sensing data, the TMDI improves the precision and reliability of drought monitoring, particularly in areas with limited ground-based observations (Le and Liou,

2021). Global warming and climate change are increasingly exacerbating drought conditions in arid and drought-prone regions, including parts of Vietnam. The impact of drought is especially severe in areas with minimal seasonal vegetation, challenging highland terrain with low water retention, and water sources that rely solely on precipitation (Le et al., 2021).

Yok Don National Park, situated in Vietnam's western Central Highlands, exemplifies these challenges. The park experiences intense solar radiation, high temperatures, and fluctuating rainfall patterns throughout different areas and seasons. It receives significant rainfall during the wet season but faces extreme precipitation deficits in the dry season (Duong and Son, 2024). These climatic factors contribute to the prevalence of deciduous dipterocarp forests (DDF), which lose their leaves in the dry season. Consequently, the park is highly vulnerable to forest fires and experiences slower recovery if the rainy season is delayed or if rainfall is reduced (Nguyen et al., 2015). This vulnerability highlights the critical need for effective drought monitoring. It is essential to evaluate how water scarcity impacts vegetation health, pinpoint at-risk areas, and develop adaptive strategies to strengthen the park's resilience to water stress. Additionally, drought monitoring supports biodiversity conservation and fosters sustainable development for local communities.

This study examines the application of the TMDI index to assess drought conditions in Yok Don National Park from 2014 to 2023 using time-series remote sensing data. By enhancing our understanding of drought trends and implementing suitable measures, this study aims to improve water resource management, mitigate ecological damage, and support this vital natural area's long-term preservation and sustainable use. The article is organized into five sections: The introduction provides the background and objectives; the second section describes the study area and datasets; the third explains the TMDI calculation method; the fourth presents and analyzes the results; and the final section summarizes the findings and conclusions.

2. Materials

2.1. Study area

Yok Don National Park, the second largest special-use forest in Vietnam, is located in the western Central Highlands, spanning from 12°45' to 13°10'N in latitudes and 107°29' to 107°48'E in longitudes. The park is approximately 38 km Northwest of Buon Ma Thuot city, primarily within Dak Lak province, with a small extension into Dak Nong province (Fig. 1). It covers a total area of 115,545 hectares, including 80,947 hectares of strictly protected area, 30,426 hectares designated for ecological restoration, and 4,172 hectares for administrative and service purposes. Additionally, a buffer zone surrounding the park encompasses 133,890 hectares, which includes the neighboring communes (EVNNPT, 2021).

Yok Don National Park is characterized by a predominantly flat landscape, with an average elevation of approximately 200 meters. The terrain also features some low hills and mountains, with Yok Don Mountain being the highest point at 482 meters (Nguyen et al., 2015). The park experiences a tropical monsoon climate, marked by a rainy season from May to October and a dry season extending from November to April of the following year. The average annual temperature ranges from 24°C to 26°C, with May being the hottest month and January the coldest. The park experiences relatively low rainfall, averaging about 1,500 mm annually (Duong and Son, 2024). Rainfall is unevenly

distributed throughout the year, peaking at 280 mm in June and typically experiencing no precipitation in January. Humidity levels in the park remain low, averaging 76% during the rainy season (https://tour.yokdonnationalpark.vn/vuon-quoc-gia-yok-don.html). The park's location deep within the Central Highlands basin contributes to its low humidity and precipitation. The eastern side is shielded by mountains ranging from 500 to 1,000 meters, while the western border is adjacent to the Cambodian mainland. This geographical setting places the park directly under the influence of the southwest monsoon, Which, when strong, creates a hot and dry climate, leading to significant water evaporation, averaging 1,078 mm annually (https://tour.yokdonnationalpark.vn/vuon-quoc-gia-yok-don.html).

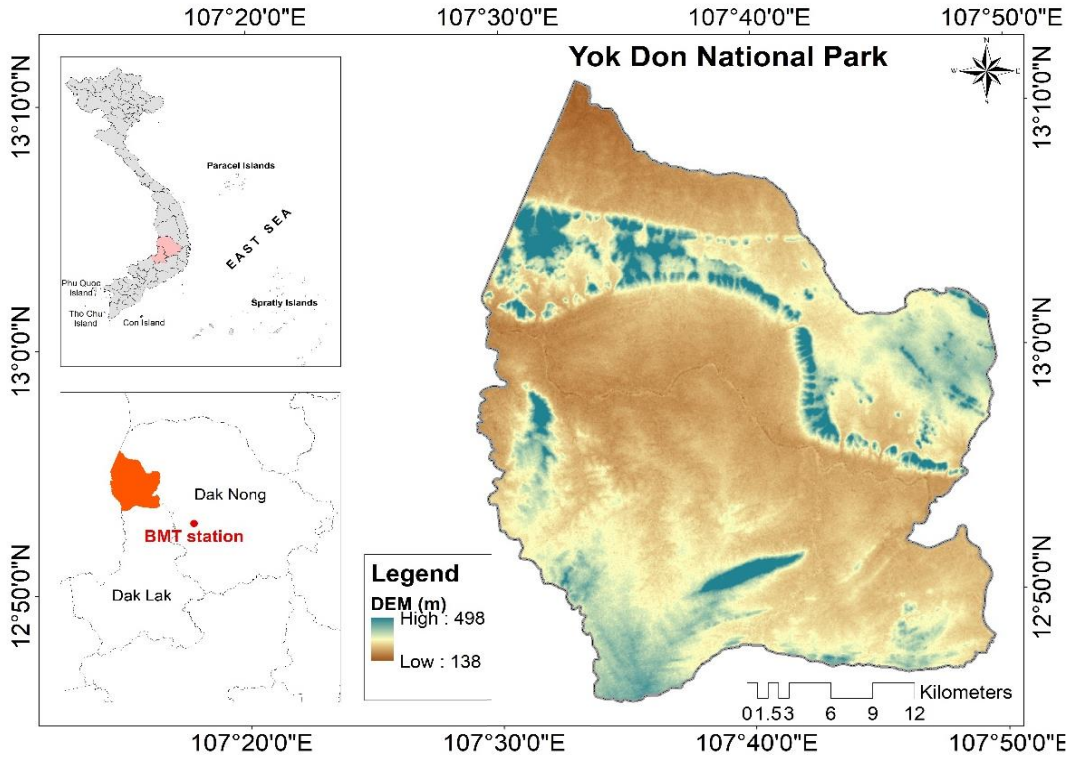

Figure 1. The location of Yok Don National Park

Yok Don National Park is renowned for its high biodiversity, hosting over 1,000 plant species and approximately 650 animal species, including numerous endemic species of flora and fauna (Cuong and Huynh, 2022). Due to its specific geographical location and climatic conditions, a distinctive dipterocarp forest ecosystem, the only one of its kind in Vietnam, has developed in the park. The park's vegetation primarily consists of deciduous and semi-evergreen forests, with evergreen forests covering smaller areas, mainly on hills and along watercourses. Yok Don National Park's topography, coupled with its consistently hot and dry climate from November to April, results in relatively sparse vegetation in the open deciduous forests. The upper tree layer, dominated by species from the Dipterocarpus family, is generally tall and sparse, featuring broad leaves that emerge

during the rainy season and shed during the dry season. These trees have developed thick, often cracked bark as an adaptation to withstand forest fires and drought. In contrast, herbaceous plants near the ground, which cannot retain water effectively, frequently wilt and are susceptible to burning during the dry season but regenerate vigorously with the onset of the rainy season. The harsh water regime results in a low density of mature woody plants, which shed their leaves during the dry season, further contributing to low vegetation cover and faster evaporation rates.

The increasing impact of climate change exacerbates drought conditions in the Central Highlands in general and Yok Don National Park in particular. The intensification and prolongation of droughts will likely disrupt habitats for both plants and animals, leading to population declines and posing a significant threat to numerous rare and endangered species. Drought monitoring is essential for evaluating the effects of water scarcity on vegetation health, identifying at-risk areas early, and devising adaptive management strategies to enhance the park's resilience to water stress. It also assists in maintaining biodiversity and promoting sustainable development for local communities.

2.2. Materials

This study focuses on monitoring drought conditions in Yok Don National Park from 2014 to 2023, utilizing the TMDI derived from satellite-based remote sensing data. The primary dataset for this analysis consists of Landsat-8 images, leveraging data from the Operational Land Imager (OLI) and Thermal Infrared Sensor (TIRS) for comprehensive monitoring. These images are particularly valuable due to their multi-spectral bands, ranging from visible to thermal infrared, enabling the calculation of spectral indices (https://www.usgs.gov/landsat-missions/landsat-8). The thermal band data from Landsat-8 is specifically used to derive LST, a crucial parameter for understanding environmental changes and drought conditions. For a comprehensive analysis, Landsat-8 OLI imagery of Yok Don National Park was systematically acquired for the dry seasons during the study period via the Google Earth Engine (GEE) platform (Pham-Duc et al., 2023). In addition, this study incorporates evapotranspiration (ET) products derived from the Moderate Resolution Imaging Spectroradiometer (MODIS) satellite data (https://modis.gsfc.nasa.gov/data/dataprod/mod16.php). These products provide valuable information on the volume of water transferred to the atmosphere from the Earth's surface through transpiration and evaporation. The MODIS ET data is instrumental in assessing the reliability and accuracy of the TMDI index for drought monitoring. ET data collection was synchronized with the acquisition of Landsat-8 OLI imagery to maintain temporal consistency. A detailed summary of the Landsat-8 OLI images and MODIS ET data utilized in this research is presented in Table 1.

To further strengthen the validation of the study's findings, precipitation data from the Buon Me Thuot meteorological station (108.050°E, 12.667°N) in Dak Lak province was acquired from 1994 to 2023. This station is significant due to its proximity to the study area and is managed by the Vietnam General Department of Meteorology and Hydrology (http://vnmha.gov.vn/). Initially collected hourly using barometers, the precipitation data were aggregated into monthly datasets. This study primarily utilizes the annual precipitation data to assess the accuracy of the TMDI in monitoring drought events.

Table 1. Details of satellite remote sensing images used in this study

Satellite sensor	Band and Descriptions		Products	Spatial resolution (m)	Temporal resolution (day)	Acquisition Date
Landsat-8 OLI, TIRS	Band 1	Coastal Aerosol	Level 2, Collection 2, Tier 1	30 × 30	16	03/03/2014 06/03/2015 08/03/2016 11/03/2017 10/02/2018 01/03/2019 03/03/2020 06/03/2021 09/03/2022 25/02/2023
	Band 2	Blue				
	Band 3	Green				
	Band 4	Red				
	Band 5	Near-Infrared				
	Band 6	SWIR 1				
	Band 7	SWIR 2				
	Band 8	Panchromatic (PAN)		15 × 15		
	Band 9	Cirrus		30 × 30		
	Band 10	TIRS 1		100 × 100		
	Band 11	TIRS 2				
MODIS	ET (Evapotranspiration)		MOD16A2GF	500 × 500	8	

3. Methodologies

3.1. Temperature-Soil Moisture Dryness Index

TMDI was proposed by Le and his team in 2021 as an indicator to assess dryness conditions across various land surface severities (Le and Liou, 2021, 2022). This index is handy in regions where temperature and surface characteristics play a significant role in determining the severity of droughts. TMDI sets itself apart by considering the relationship between NDLI and LST and their fluctuations. It recognizes that while temperature offers a time-sensitive indication of surface water, relying solely on temperature for monitoring water scarcity might be influenced by varying water features across different land covers. By incorporating NDLI and surface temperature, TMDI enhances the effectiveness of surface dryness monitoring, taking advantage of the sensitivity of visible, shortwave-infrared, and thermal infrared bands to water, which, in turn, expands its applicability.

Instead of treating LST and NDLI as independent measurements, TMDI leverages their correlation, which is visually represented through a scatter plot within a triangular space on a two-dimensional coordinate system. This triangular space represents three distinct conditions: the upper left corner denotes arid areas with sparse vegetation, characterized by low NDLI values and high LST values; the lower left corner signifies regions with moist soil, indicated by low values for both NDLI and LST; and the bottom right corner reflects areas with high moisture content and abundant water availability, depicted by high NDLI values and low LST values (Le et al., 2023). This connection between LST and NDLI can be mathematically expressed through the TMDI formula as follows:

$$TMDI = (LST_s - LST_{min})/(LST_{max} - LST_{min}) \quad (1)$$

LSTs denote a specific pixel's surface temperature value (°C), and LST_{max} and LST_{min} correspond to the highest and lowest surface temperatures observed among pixels sharing identical surface conditions (i.e., a uniform NDLI value).

To build this formula, LST and NDLI are combined first to determine the highest and lowest surface temperature values for distinct surface conditions, all within a small range of NDLI. Linear fits are then applied to the NDLI data, resulting in equations for the dry edge (Eq. 2) and the wet edge (Eq. 3) within the defined feature space.

$$LST_{min} = a_1 + b_1 * NDLI \quad (2)$$

$$LST_{max} = a_2 + b_2 * NDLI \quad (3)$$

Here, a_1, b_1, and a_2, b_2 represent the coefficients of the wet and dry edge equations, respectively.

3.2. Land Surface Temperature

Land surface temperature data for Yok Don National Park, spanning the period from 2014 to 2023, was derived from Landsat 8 OLI-TIRS Collection 2 Level 2 datasets using the GEE platform (https://developers.google.com/earth-engine/datasets/catalog/LANDSAT_LC08_C02_T1_L2). These datasets were produced from Landsat Collection 2 Level-1 thermal infrared bands and supplemented with additional information such as Top of Atmosphere (TOA) reflectance, TOA Brightness Temperature, data from the Advanced Spaceborne Thermal Emission and Reflection Radiometer (ASTER) Global Emissivity Database (GED), NDVI, and atmospheric profiles encompassing parameters such as geopotential height, specific humidity, and air temperature (Jimenez-Munoz et al., 2014; Ru et al., 2021).

3.3. Normalized Difference Latent Heat Index

The Normalized Difference Latent Heat Index (NDLI) was developed to assess latent heat flux and surface water presence. It involves combining spectral data from band 3 (Green), band 4 (Red), and band 6 (Shortwave Infrared - SWIR 1) of Landsat imagery to calculate NDLI (Liou et al., 2019). The NDLI is formulated as in equation (4):

$$NDLI = (\mathrm{B3} - \mathrm{B4})/(\mathrm{B3} + \mathrm{B4} + \mathrm{B6}) \quad (4)$$

where B3, B4, and B6 correspond to the Green, Red, and SWIR1 bands of Landsat 8 OLI dataset, respectively.

3.4. Validation

Evapotranspiration (ET), a key metric for assessing surface water availability, plays a vital role in drought evaluation. ET provides valuable information on the volume of water transferred to the atmosphere from the Earth's surface through transpiration and evaporation. During periods of drought, reduced rainfall lowers soil moisture, causing ET rates to surpass precipitation levels. This imbalance results in water stress for plants and ecosystems. Consequently, areas with low ET values can be considered drier than those with higher ET values. As a result, ET values play a crucial role in drought monitoring studies and have been widely used as reference data to validate the accuracy of drought analysis results (Maes and Steppe, 2012; Nguyen et al., 2024). In this study, ET data, synchronized with the acquisition of Landsat-8 OLI imagery, were used to evaluate the effectiveness of TMDI in drought assessment during the selected period in Yok Don National Park.

A resizing technique is implemented to upscale the 30-meter resolution TMDI maps to a 500-meter resolution, aligning them with the ET product maps. This technique aggregates pixels with smaller spatial resolutions into pixels with larger resolutions using statistical methods. From the 30 m resolution TMDI dataset, which falls within the coverage of a 500 m resolution ET pixel, statistical measures such as the mean, median, or mode can be used to represent the new 500 m resolution TMDI pixel. In this study, the mean value was selected. To automate the processing workflow, the "image.reduceResolution(.)" function, provided by the GEE platform, was utilized to generate 500 m resolution TMDI maps, enabling correlation analysis between TMDI and ET. Details of this technique can be found at the following link: https://developers.google.com/earth-engine/guides/resample. The 500 m resolution TMDI maps will be presented in Figure A-1 of the appendix.

A workflow was proposed to follow the calculation process easily, as presented in Fig. 2.

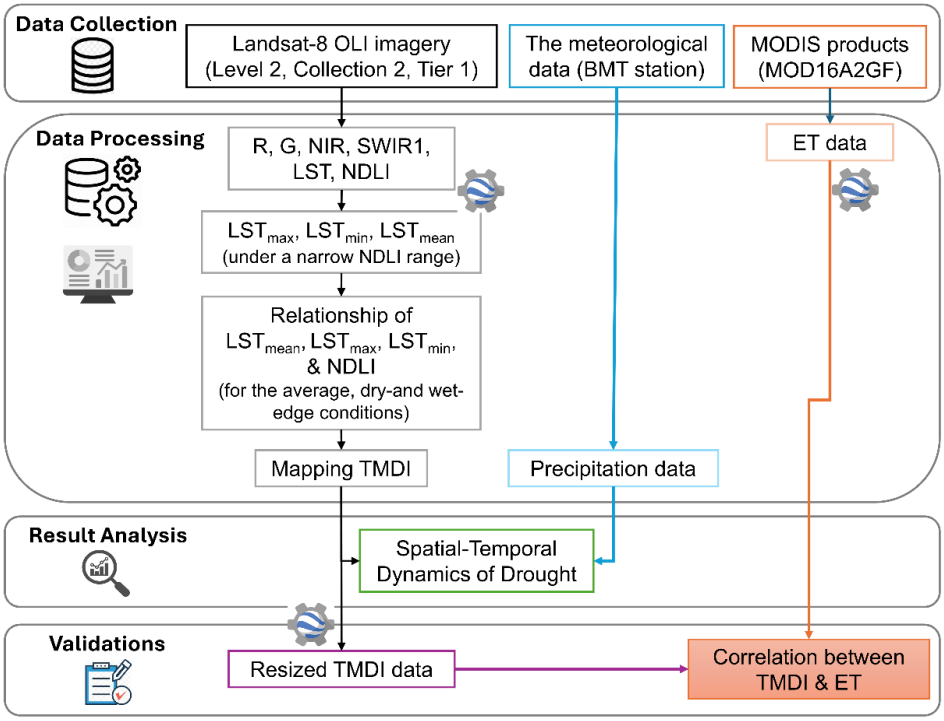

Figure 2. The workflow for investigating the spatiotemporal dynamics of drought over Yok Don National Park using TMDI

4. Results & Discussion

4.1. LST & NDLI correlation

This study examined the association between land surface temperature and water availability across various land cover types, as represented by the NDLI. Initially, samples were gathered to establish the connection between NDLI and LST at the dry and wet edges. Within this process, each 0.05 interval of NDLI was considered representative of a specific surface condition, and all LTS data within the selected NDLI range were included. To minimize the influence of outliers, only LST values that corresponded to the selected NDLI range and adhered to the principles of normal distribution statistics were retained, specifically, as in equations (5) and (6):

$$|LST_i - \overline{LST}| \leq 3.5\ \sigma_{LST} \quad if\ n > 2000 \qquad (5)$$

$$|LST_i - \overline{LST}| \leq 3\ \sigma_{LST}\ if\ 300 \leq n < 2000 \qquad (6)$$

where $\overline{LST}$ and σ_{LST} are the mean and standard deviation of the land surface temperature, respectively, for a specific surface condition represented by a selected range of NDLI; n is the number of LST values within this range.

Samples are excluded when the number of LST observations is fewer than 300. Finally, the values of NDLI, LST_{max}, LST_{min}, and LST_{mean} are used to determine the coefficients in equations (2) and (3). The correlations between LST and NDLI were analyzed for 2014–2023 using a triangular/trapezoidal space (Fig. 3). In each panel of Fig. 3, dot colors represent the density of specific surface conditions linked to water availability and temperature. For a narrow NDLI range indicating a particular water availability, the upper black triangle with high LST signifies dry conditions.

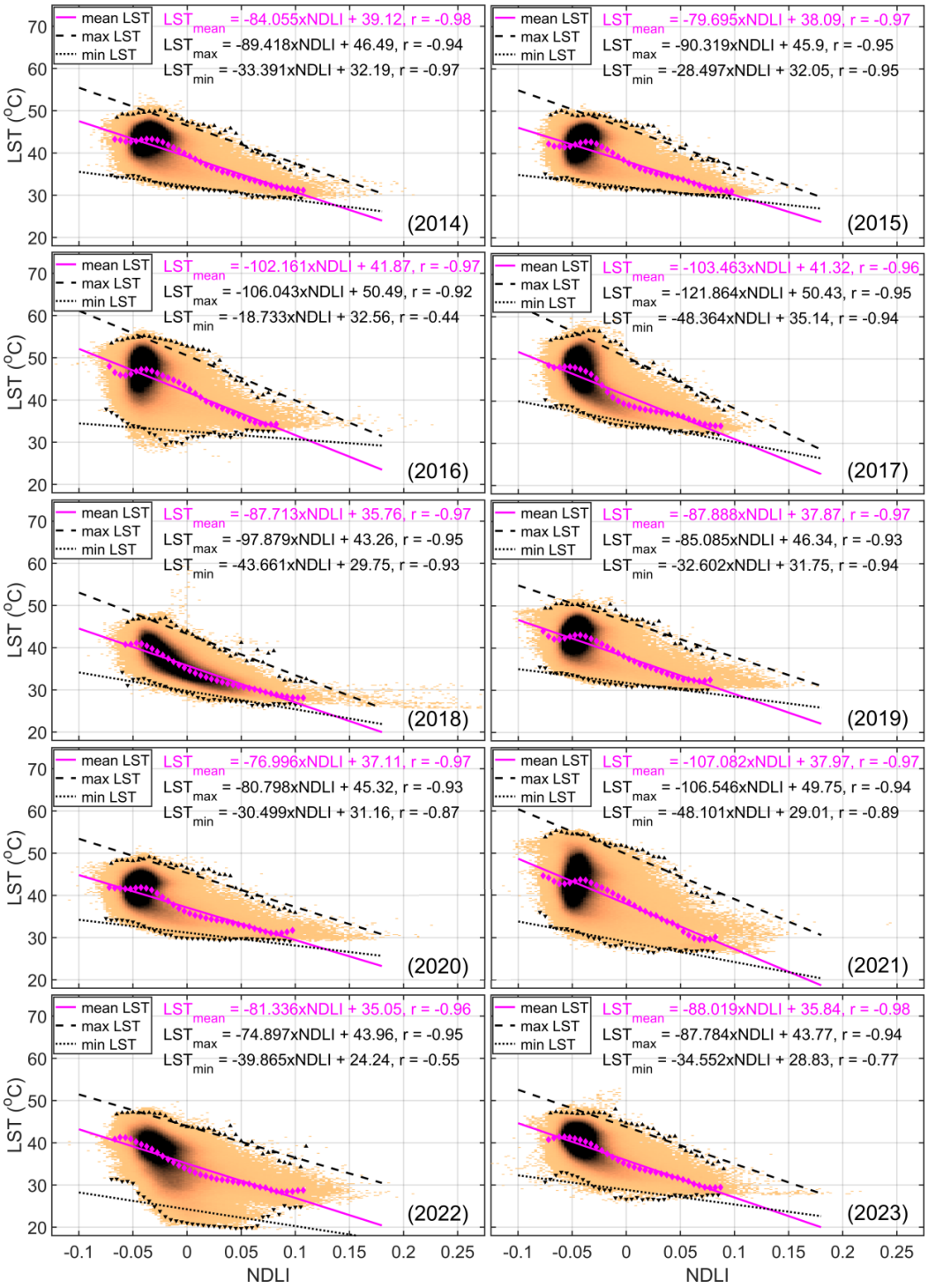

Figure 3. Scatter plots show the relationship between NDLI and LST over Yok Don National Park during the dry season from 2014 to 2023

In contrast, the lower black triangle with low LST indicates wet conditions. Magenta diamonds represent the mean LST, reflecting average surface conditions. The magenta solid line, black dashed line, and black dotted line correspond to the regression lines for each year's average, dry-edge, and wet-edge conditions of the land surface, respectively. Text annotations on the panels provide the parameters of the three linear regression models and their corresponding correlation values.

The results revealed consistent negative correlations between LST and NDLI, suggesting that higher water availability corresponds to lower surface temperatures. This provides significant insights into how different land cover types influence surface temperatures about water availability. Furthermore, the analysis showed that LST exhibits consistent fluctuations within specific NDLI value ranges. ‘‘Dry points” displayed higher LST, whereas “wet points” exhibited lower LST. This observation implies that land cover properties play a crucial role in modulating the impact of water content on surface temperatures. Significant correlations were observed between LST and NDLI along the dry edge, indicating that regions experiencing higher temperatures exhibit a stronger relationship between temperature and water content. This suggests that variations in water availability more profoundly affect surface temperatures in areas with elevated temperatures. This finding is particularly valuable for understanding the interplay between land surface temperature and water availability across diverse land cover types.

In each panel, the color of each dot represents the density of specific surface conditions associated with existing water availability and temperature. For a small NDLI range representing a particular level of surface water availability, the upper black triangle with high LST indicates dry conditions. In contrast, the lower black triangle with low LST represents wet conditions. Magenta diamonds denote the mean LST, indicating the average surface conditions. The magenta solid line, black dashed line, and black dotted lines represent the regression lines for the land surface's average, dry-edge, and wet-edge conditions, respectively, for each year.

4.2. Drought distribution

By TMDI’s principle, its values range from 0 to 1, where 1 corresponds to the dry edge, and 0 signifies the wet edge (Le and Liou, 2022). Higher TMDI values reflect more severe drought conditions, while lower values suggest milder surface droughts. Within the LST-NDLI feature space, the triangular framework illustrates three distinct scenarios: First, the upper left corner represents arid conditions with barren soil, characterized by low NDLI and high LST values; second, the lower left space signifies moist soil conditions, marked by both NDLI and LST values at their minimum; and lastly, the bottom right space indicates saturated soil with the highest water availability, exemplified by high NDLI values and low LST values.

In areas of bare soil, surface temperature changes are strongly linked to variations in water availability. As one moves from the top-left to the bottom-left corner of the triangular feature space, water exchange via evapotranspiration gradually increases, reflecting a transition from minimal to maximal interaction between the surface and the atmosphere. The bottom-right region exhibits abundant surface water availability, corresponding to a water stress index 0. The oblique side of the triangle represents the "dry edge," characteristic of drought conditions, whereas the triangle's base signifies a "wet edge" state, indicative of saturated soil conditions.

To monitor drought in the Yok Don National Park, the TMDI maps were generated specifically for the dry seasons from 2014 to 2023 (Fig. 4). The

comprehensive analysis of these maps revealed a clear pattern illustrating the evolution of drought conditions over the years. Initially, there was a noticeable uptick in drought severity starting in 2014, intensifying further in 2015, and reaching its peak in 2016, marking the most extreme drought during the study period. This observation is consistent with reports of a worsening drought crisis and widespread water shortages across the Central Highlands region, particularly in areas cultivating perennial industrial crops like coffee and black pepper. Approximately 70% of rainfed or minimally irrigated agricultural land was severely affected, with 7,100 hectares abandoned and over 95,000 hectares experiencing irrigation deficiencies (CCAFS-SEA, 2016). Following the severe drought in 2016, dry areas were reduced between 2017 and 2020. However, signs of worsening drought conditions reappeared in 2021, persisted through 2022, and began to diminish by 2023.

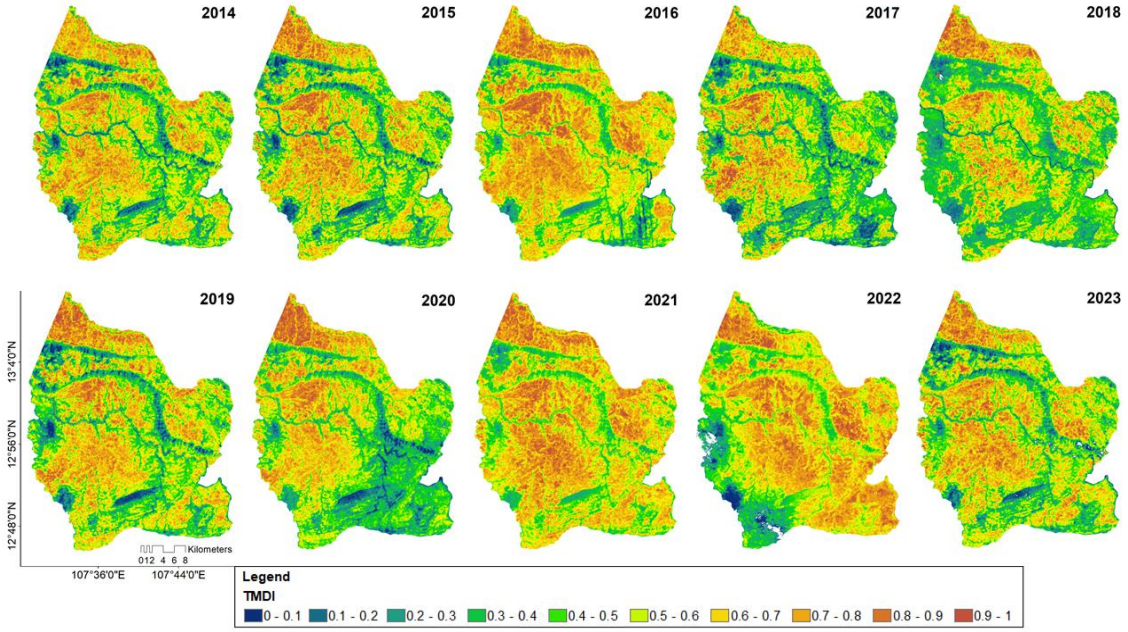

Figure 4. The spatial distribution of TMDI over Yok Don National Park during the middle of the dry season from 2014 to 2023

The varying patterns of drought conditions, as revealed by the TMDI maps, highlight the intricate interactions among diverse climatic factors. Due to the absence of meteorological stations within the Yok Don National Park, precipitation data from the nearest available station, Buon Ma Thuot (BMT), was utilized to validate the results obtained from the TMDI index regarding drought occurrences. The findings indicate that the drought patterns identified by TMDI align with the trends observed in actual precipitation data collected from the BMT meteorological station. Annual rainfall figures from 2013 to 2023, ranging from 1,511.9 to 2,108 mm per year, illustrate the fluctuating nature of precipitation in the region (Fig. 5). An analysis of rainfall trends recorded at the BMT station revealed two distinct periods of decreasing precipitation, notably in 2015 and 2016, followed by another decline in 2022. This temporal analysis strongly supports the reliability of the TMDI index in identifying drought periods in the study area.

The TMDI maps, shown in Fig. 4, focus on Yok Don National Park, offering crucial

insights into drought occurrences during the middle dry season from 2014 to 2023. Spatial analysis reveals significant drought characteristics across the study area, with notable interannual variations in the extent of drought-affected surface areas, particularly in 2016, 2021, and 2022. The northern and central regions of the park consistently experienced severe drought impacts throughout the study period. To better understand the relationship between drought and land cover characteristics, the land cover maps adopted from previous research by Nguyen et al. (2015, 2017) were used to analyze drought patterns across different forest systems. The findings revealed that drought-prone areas predominantly correspond to regions covered by poor- to medium-density deciduous dipterocarp forests, as shown in Figure A-2. Conversely, areas with low TMDI values are situated at higher-altitude locations, characterized by dense evergreen broadleaf forests. In other regions, including the east, southeast, and southwest areas, TMDI trends varied over the years. This variability arises from the mosaic composition of evergreen broadleaf and rich deciduous dipterocarp forests in these areas. Vegetation in these regions tends to remain lush following years of abundant rainfall but may become arid when rainfall in the preceding year is insufficient, as illustrated in Fig. 5.

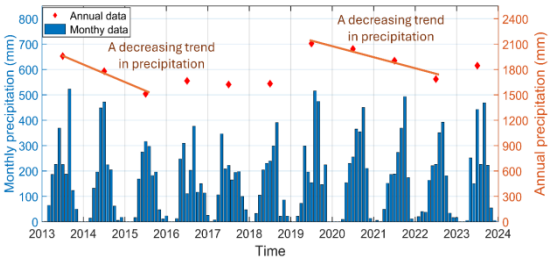

Figure 5. Variations in precipitation were recorded at the Buon Ma Thuot (BMT) meteorological station, the closest station to Yok Don National Park. Blue dots and red diamonds represent monthly and annual precipitation data from 2013 to 2023

Furthermore, this study highlights the critical role of forest ecosystems in shaping drought dynamics. Deciduous broadleaf forests are particularly susceptible to drought due to their seasonal leaf-shedding behavior, which limits their ability to retain moisture. In contrast, evergreen forests, with their multiple canopy layers and high water-holding capacity, exhibit greater resilience to drought. Additionally, the uppermost canopy leaves of evergreen trees utilize water more conservatively than those of drought-deciduous trees (Ishida et al., 2013). As a result, regions dominated by deciduous trees are more vulnerable to water scarcity, reinforcing the finding that drought primarily affects areas covered by deciduous broadleaf forests.

These findings are crucial for identifying conservation areas highly vulnerable to drought. They provide a foundation for targeted interventions, such as reforestation, water conservation, forest fire prevention, and adaptive management strategies, particularly in deciduous dipterocarp forests, prone to drought and at risk of burning due to their limited water retention capacity. By understanding the spatial distribution of drought impacts, park managers can enhance ecosystem resilience, preserve biodiversity, and maintain the park's ecological functions. In the face of climate change, this work supports sustainable forest management and long-term conservation planning.

4.3. Validation

Given the absence of ground-based measurements within the study area, this study utilized NASA's ET products as reference data to assess the effectiveness of TMDI in evaluating water deficit dynamics (Fig. 6). The ET values used in this study were averaged from MODIS-derived products over the first three months of each year, corresponding to the mid-dry season in

Yok Don National Park. During this period, rainfall is minimal, and drought conditions peak. The Landsat-8 OLI images were captured in late February or early March, when drought conditions are most severe, significantly affecting vegetation responses. Observations of temperature and water availability on the surface reflect the cumulative effects of prolonged drought since the onset of the dry season. Therefore, averaging ET values over the first three months of the year reduces short-term fluctuation noise and enhances the reliability and objectivity of the research findings. This approach provides a more accurate representation of drought impacts on vegetation as reflected by the TMDI index.

To address the spatial resolution mismatch between the TMDI maps and ET products, the resizing technique presented in the methodology section is applied to upscale the 30-meter TMDI maps to a 500-meter resolution (Figure A-1), aligning them with the ET product maps. Subsequently, the correlation between TMDI and ET is analyzed based on randomly selected points. The computed correlation coefficients are presented in Fig. 7, demonstrating a consistent inverse relationship between TMDI values and ET rates. Specifically, correlation coefficients ranging from -0.55 to -0.70 were observed between TMDI and three-month ET data throughout the study period from 2014 to 2023. These stable negative correlations between TMDI-derived drought assessments and actual ET rates highlight the effectiveness of TMDI in accurately capturing land surface water availability.

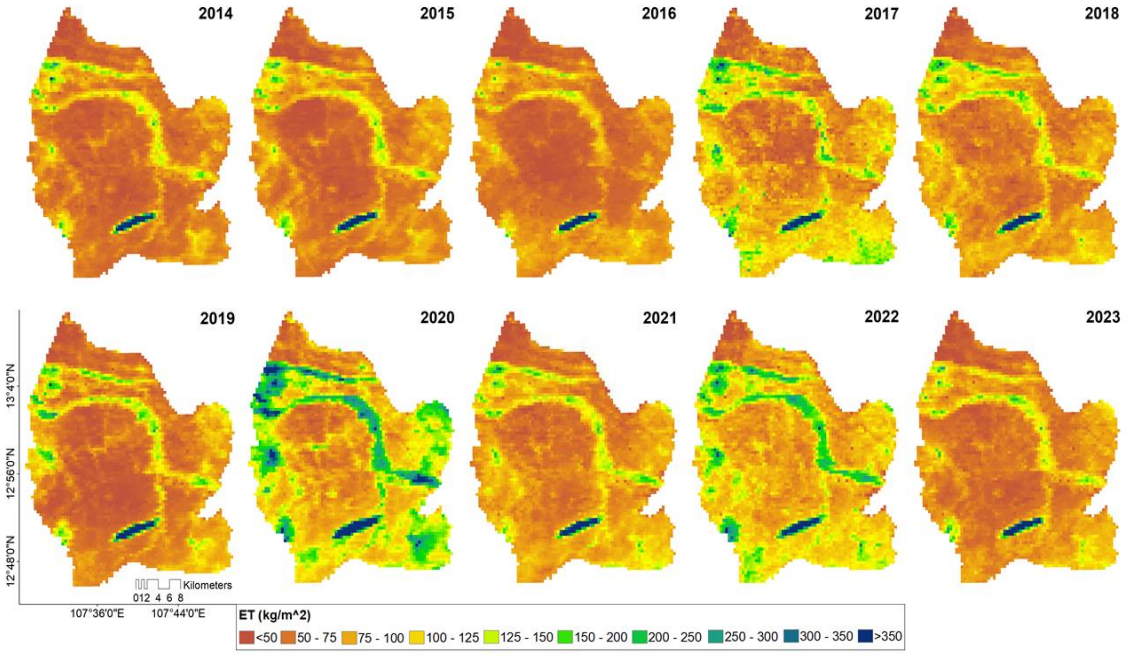

Figure 6. The spatial distribution of average ET, calculated from MODIS-derived products over Yok Don National Park, represents the mean values for the first three months of each year during the mid-dry season from 2014 to 2023

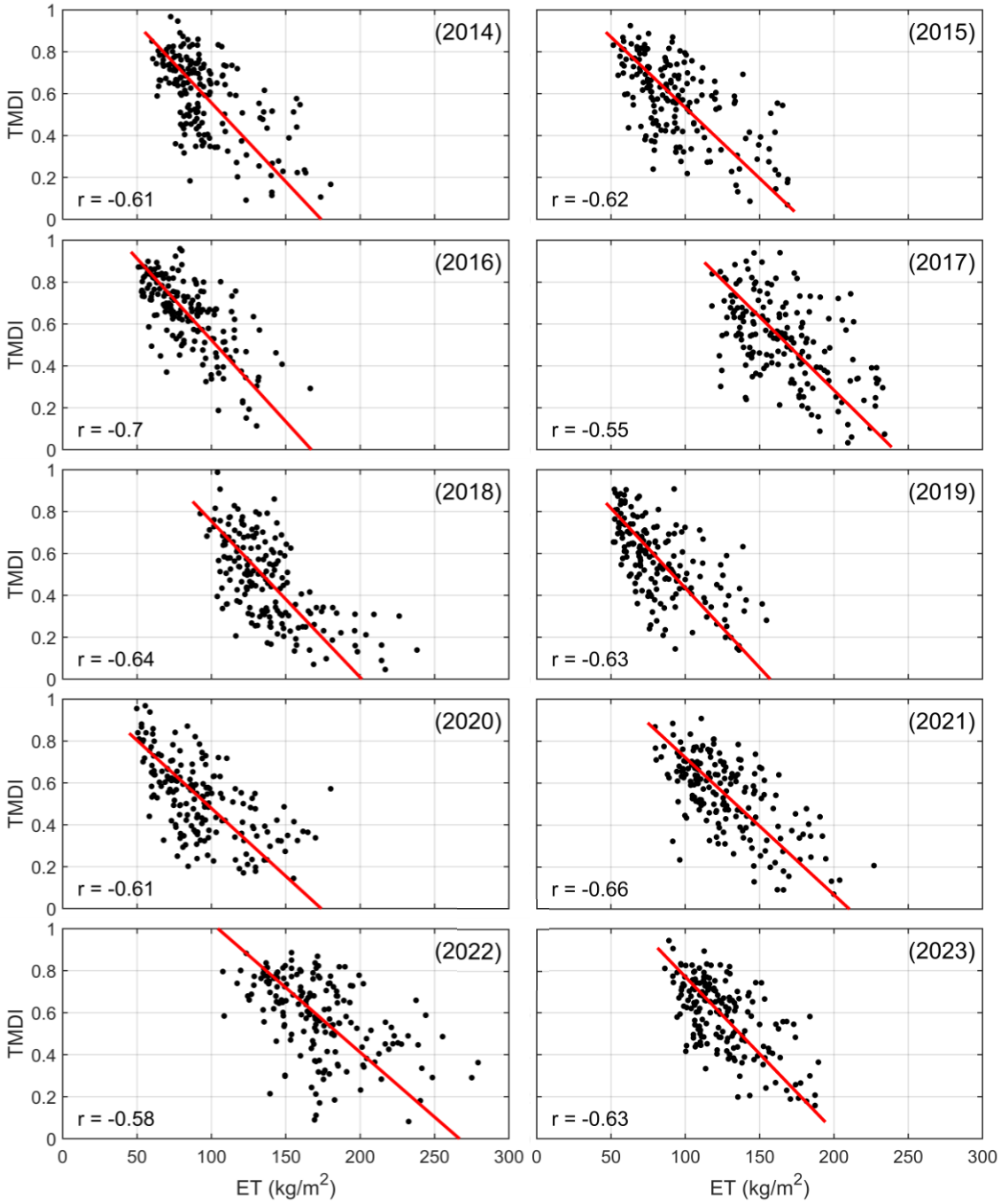

Figure 7. The correlation coefficients between ET and TMDI from 2014 to 2023. In each panel, black dots represent the ET and TMDI values at the same location, and the red line shows the linear regression model between these two variables. *r* stands for the correlation coefficient, and the accompanying number represents its value

The negative correlations in Fig. 7 suggest that during periods identified by the TMDI as drought-prone, there are concurrent declines in ET values. The sensitivity of TMDI to fluctuations in land cover water content due to water scarcity is prominently evidenced by its consistent negative association with the process of water moving from the surface to the atmosphere. This indicates that TMDI effectively captures the reduction in water availability across the Yok Don National Park landscape during drought periods. The effectiveness of TMDI in reflecting how the Earth's surface reacts to drought events is highlighted by its ability to capture the intricate interplay between precipitation and water exchange between land and air. TMDI effectively reflects changes in water availability and corresponds with observed variations in evapotranspiration, offering a deeper insight into drought dynamics. This demonstrates the efficiency of TMDI in capturing variations in surface water availability. By providing a quantitative measure of drought severity and its spatial distribution, TMDI serves as a valuable tool for informing drought monitoring and management efforts in Yok Don National Park and other regions facing water scarcity challenges.

5. Conclusions

This study successfully employed the Temperature-Moisture Drought Index to assess drought conditions in Yok Don National Park from 2014 to 2023 using remote sensing data. The study provided a detailed understanding of drought dynamics across various land cover types by analyzing the relationship between land surface temperature and water availability represented by the Normalized Difference Latent Heat Index.

The results revealed a gradual escalation in drought severity beginning in 2014, peaking in 2016 with the most severe drought of the study period. A subsequent decrease in drought intensity was observed from 2017 to 2020, followed by escalating dry conditions from 2021 to 2022, which then moderated by 2023. The drought trends identified by the TMDI index were consistent with actual precipitation data collected from a nearby meteorological station. Additionally, the results demonstrated differences in water scarcity among various forest types. The findings indicated that severe drought impacts were predominantly observed in areas covered by deciduous broadleaf forests, which naturally shed leaves during the dry season. In contrast, evergreen broadleaf forests exhibited greater drought resilience.

Furthermore, the surface evapotranspiration rate, a reliable indicator of surface water availability and a key factor in drought assessment was used to validate the effectiveness of TMDI. The analysis revealed a consistent negative correlation between TMDI values and land surface evapotranspiration rates, with correlation coefficients ranging from -0.55 to -0.70. This finding confirms that TMDI is an effective tool for accurately capturing land surface water availability and assessing drought conditions. In conclusion, the application of TMDI in this study provided a reliable and detailed assessment of drought patterns, offering valuable insights for drought monitoring and management efforts in Yok Don National Park and other regions facing water scarcity challenges.

Acknowledgments

This work was supported by the Vietnam Academy of Science and Technology, project number VAST08. 01/25-26. Satellite data are supported by the United States Geological Survey (USGS); satellite scenes were accessed and processed within the Google Earth Engine environment (source code: https://code.earthengine.google.com/11af9ae328c9b8a62a9f46a94f1e5cde).

References

Asefjah B., Fanian F., Feizi Z., Abolhasani A., Paktinat H., Naghilou M., Cabello D., Asadollahi M., Babakhani M., Salehi F., Kourosh Niya A., 2014. Meteorological drought monitoring using several drought indices (case study: Salt Lake Basin in Iran). Desert, 19, 155–165. Doi: 10.22059/JDESERT.2014.52344.

Belal A.A., El-Ramady H.R., Mohamed E.S., Saleh A.M., 2014. Drought risk assessment using remote sensing and GIS techniques. Arab. J. Geosci., 7, 35–53. https://doi.org/10.1007/s12517-012-0707-2.

Cai S., Zuo D., Wang H., Xu Z., Wang G.Q., Yang H., 2023. Assessment of agricultural drought based on multi-source remote sensing data in a major grain producing area of Northwest China. Agric. Water Manag., 278, 108142. https://doi.org/10.1016/j.agwat.2023.108142.

CCAFS-SEA, 2016. The drought crisis in the Central Highlands of Vietnam. url: https://cgspace.cgiar.org/rest/bitstreams/78532/retrieve.

Das A.C., Shahriar S.A., Chowdhury M.A., Hossain M.L., Mahmud S., Tusar M.K., Ahmed R., Salam M.A., 2023. Assessment of remote sensing-based indices for drought monitoring in the north-western region of Bangladesh. Heliyon, 9(2), 1–14. https://doi.org/10.1016/j.heliyon.2023.e13016.

EVNNPT, 2021. Environmental and Social Management Framework (ESMF). url: http://www.sppmb.npt.evn.vn/wp-content/uploads/2021/04/ESMF_P174460-REACH_14-Apr-2021.pdf.

Fung K., Huang Y., Koo C., Soh Y., 2020. Drought forecasting: A review of modelling approaches 2007–2017. J. Water Clim. Change., 11(3), 771–799. https://doi.org/10.2166/wcc.2019.236.

Gu Y., Brown J.F., Verdin J.P., Wardlow B., 2007. A five-year analysis of MODIS NDVI and NDWI for grassland drought assessment over the central Great Plains of the United States. Geophys. Res. Lett., 34(6), L06407. https://doi.org/10.1029/2006GL029127.

Ishida A., Yamazaki J.-Y., Harayama H., Yazaki K., Ladpala P., Nakano T., Adachi M., Yoshimura K., Panuthai S., Staporn D., Maeda T., Maruta E., Diloksumpun S., Puangchit L., 2013. Photoprotection of evergreen and drought-deciduous tree leaves to overcome the dry season in monsoonal tropical dry forests in Thailand. Tree Physiol., 34(1), 15–28. Doi: 10.1093/treephys/tpt107.

Jimenez-Munoz J.C., Sobrino J.A., Skoković D., Mattar C., Cristobal J., 2014. Land surface temperature retrieval methods from Landsat-8 thermal infrared sensor data. IEEE Geosci. Remote Sens. Lett., 11(10), 1840–1843. Doi: 10.1109/LGRS.2014.2312032.

Le Mai Son, Liou Y.A., 2021. Spatio-Temporal Assessment of Surface Moisture and Evapotranspiration Variability Using Remote Sensing Techniques. Remote Sens., 13(9), 1667. https://doi.org/10.3390/rs13091667.

Le Mai Son, Liou Y.A., 2022. Temperature-Soil Moisture Dryness Index for Remote Sensing of Surface Soil Moisture Assessment. IEEE Geosci. Remote Sens. Lett., 19, 1–5. Doi: 10.1109/LGRS.2021.3095170.

Le Mai Son, Liou Y.A., Pham M.T., 2023. Crop Response to Disease and Water Scarcity Quantified by Normalized Difference Latent Heat Index. IEEE Access, 11, 55938–55946. Doi: 10.1109/ACCESS.2023.3283033.

Le Tien, Sun C., Choy S., Kuleshov Y.J.G., 2021. Regional drought risk assessment in the Central Highlands and the South of Vietnam. Geomatics Nat. Hazards Risk., 12(1), 3140–3159. Doi: 10.1080/19475705.2021.1998232.

Lesk C., Rowhani P., Ramankutty N., 2016. Influence of extreme weather disasters on global crop production. Nature 529, 84–87. https://doi.org/10.1038/nature16467.

Liou Y.A., Le Mai Son, Chien H., 2019. Normalized Difference Latent Heat Index for Remote Sensing of Land Surface Energy Fluxes. IEEE Trans. Geosci. Remote Sens., 57(3), 1423–1433. Doi: 10.1109/TGRS.2018.2866555.

Maes W.H., Steppe K., 2012. Estimating evapotranspiration and drought stress with ground-based thermal remote sensing in agriculture:

a review. J. Exp. Bot., 63(13), 4671–4712. Doi: 10.1093/jxb/ers165.

Mishra A.K., Ines A.V., Das N.N., Khedun C.P., Singh V.P., Sivakumar B., Hansen J.W., 2015. Anatomy of a local-scale drought: Application of assimilated remote sensing products, crop model, and statistical methods to an agricultural drought study. J. Hydrol., 526, 15–29. https://doi.org/10.1016/j.jhydrol.2014.10.038.

MONRE, 2019. Vietnam national communi cation submission 3 to the United nations framework convention on climate change. Vietnam: Ministry of Natural Resources and Environment. url: https://unfccc.int/documents/192805.

Mullapudi A., Vibhute A.D., Mali S., Patil C.H., 2023. A review of agricultural drought assessment with remote sensing data: methods, issues, challenges and opportunities. Appl. Geomatics, 15(1), 1–13. https://doi.org/10.1007/s12518-022-00484-6.

Nguyen Manh Hung, Dao Duy Toan, Le Mai Son, Le Trung Hung, 2024. A modification of normalized difference drought index to enhance drought assessment using remotely sensed imagery. Environ. Monit. Assess., 196(10), 883. Doi: 10.1007/s10661-024-13060-9.

Nguyen Thuy Cuong, Huynh Van Chuong, Luu The Anh, 2022. Environmental Efficiency of Dipterocarp forest land management at Yok Don National Park. Hue Univ. J. Sci.: Agric. Rural Dev., 131(3C), 65–82. https://doi.org/10.26459/hueunijard.v131i3C.6992.

Nguyen Viet Luong, Ryutaro T., Akihiko K., Ngo Duc Anh, Nguyen Thanh Loan, Luu The Anh, 2017. Land cover mapping in Yok Don National Park, Central Highlands of Viet Nam using Landsat 8 OLI images. Vietnam J. Earth Sci., 39(4), 393–406. Doi: 10.15625/0866-7187/39/4/10773.

Nguyen Viet Luong, Ryutaro T., Nguyen Thanh Hoan, To Trong Tu, 2015. Forest change and its effect on biomass in Yok Don National Park in Central Highlands of Vietnam using ground data and geospatial techniques. Adv. Remote Sens., 4(2), 108–118. Doi: 10.4236/ars.2015.42010.

Nguyen Viet Luong, Ryutaro T., Nguyen Thanh Hoan, To Trong Tu, Le Mai Son, 2015. An analysis of forest biomass changes using geospatial tools and ground survey data: a case study in Yok Don national park, Central Highlands of Vietnam. Vietnam J. Earth Sci., 36(4), 439–450. https://doi.org/10.15625/0866-7187/36/4/6432.

Pham-Duc Binh, Nguyen Ho, Phan Hien, Tran-Anh Quan, 2023. Trends and applications of google earth engine in remote sensing and earth science research: a bibliometric analysis using scopus database. Earth Sci. Inform., 16(3), 2355–2371. Doi: 10.1007/s12145-023-01035-2.

Philip S.Y., Kew S.F., van der Wiel K., Wanders N., Jan van Oldenborgh G., 2020. Regional differentiation in climate change induced drought trends in the Netherlands. Environ. Res. Lett., 15(9), 094081. Doi: 10.1088/1748-9326/ab97ca.

Phung Thai Duong, Do Xuan Son, 2024. Assessing forest changes in Yok Don National Park and surrounding areas, Dak Lak province, Vietnam. J. Degrad. Min. Lands Manag., 11(2), 5521–5531. Doi: 10.15243/jdmlm.2024.112.5521.

Ru C., Duan S.B., Jiang X.G., Li Z.L., Jiang Y., Ren H., Leng P., Gao M., 2021. Land surface temperature retrieval from Landsat 8 thermal infrared data over urban areas considering geometry effect: Method and application. IEEE Trans. Geosci. Remote Sens., 60, 1–16. Doi: 10.1109/TGRS.2021.3088482.

Sandholt I., Rasmussen K., Andersen J., 2002. A simple interpretation of the surface temperature/vegetation index space for assessment of surface moisture status. Remote Sens. Environ., 79(2), 213–224. https://doi.org/10.1016/S0034-4257(01)00274-7.

Shahabfar A., Eitzinger J., 2013. Spatio-Temporal Analysis of Droughts in Semi-Arid Regions by Using Meteorological Drought Indices. Atmosphere, 4(2), 94–112. https://doi.org/10.3390/atmos4020094.

UNDP, 2016. Vietnam drought and saltwater intrusion: Transitioning from emergency to recovery. url: https://www.undp.org/sites/g/files/zskgke326/files/migration/vn/Recovery-draft-Sep-2016_final.pdf.

UNESCAP, 2019. Ready for the dry years: building resilience to drought in Southeast Asia. url: https://repository.unescap.org/handle/20.500.12870/3003.

Van Hoek M., Jia L., Zhou J., Zheng C., Menenti M., 2016. Early Drought Detection by Spectral Analysis of Satellite Time Series of Precipitation and Normalized Difference Vegetation Index (NDVI). Remote Sens., 8, 422. https://doi.org/10.3390/rs8050422.

Vicente-Serrano S.M., Cabello D., Tomás-Burguera M., Martín-Hernández N., Beguería S., Azorin-Molina C., Kenawy A.E., 2015. Drought Variability and Land Degradation in Semiarid Regions: Assessment Using Remote Sensing Data and Drought Indices (1982–2011). Remote Sens., 7(4), 4391–4423. https://doi.org/10.3390/rs70404391.

Wilhite D., Glantz M., 1985. Understanding: the Drought Phenomenon: The Role of Definitions. Water Int., 10, 111–120. https://www.tandfonline.com/doi/pdf/10.1080/02508068508686328.

World Bank, 2021. Climate Risk Country Profile: Vietnam. url: https://climateknowledgeportal.worldbank.org/sites/default/files/2021-04/15077-Vietnam%20Country%20Profile-WEB.pdf.

Zhang S., Wu Y., Sivakumar B., Mu X., Zhao F., Sun P., Sun Y., Qiu L., Chen L., Meng X., Han J., 2019. Climate change-induced drought evolution over the past 50 years in the southern Chinese Loess Plateau. Environ. Model. Softw., 122, 104519. https://doi.org/10.1016/j.envsoft.2019.104519.

Zhong R., Chen X., Lai C., Wang Z., Lian Y., Yu H., Wu X., 2019. Drought monitoring utility of satellite-based precipitation products across mainland China. J. Hydrol., 568, 343–359. https://doi.org/10.1016/j.jhydrol.2018.10.072.s.

Appendix

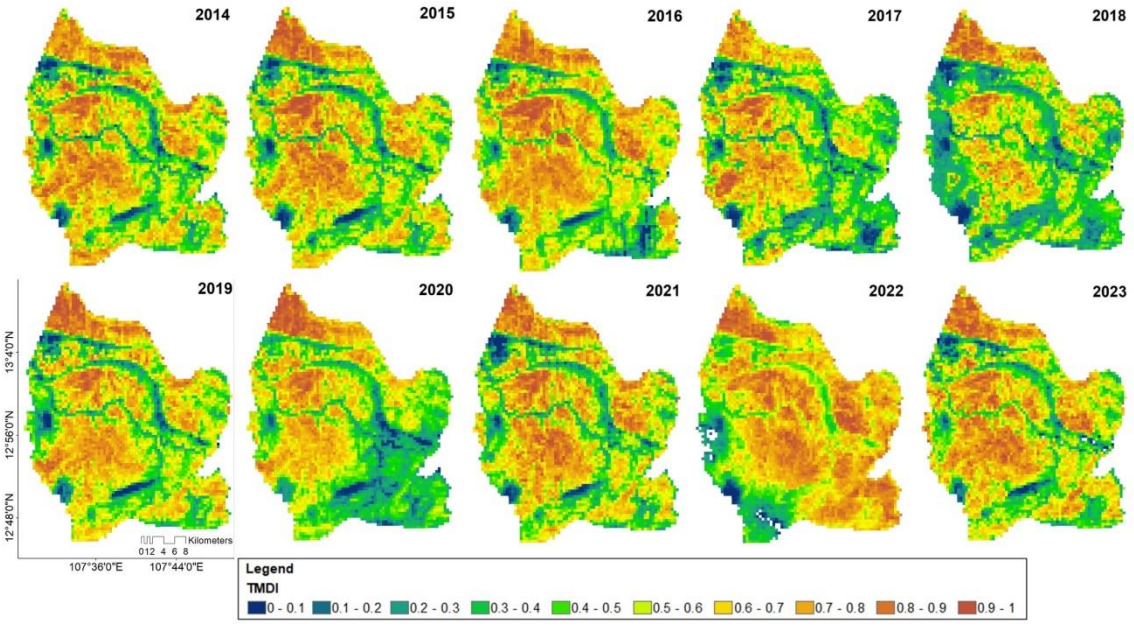

Figure A-1. Resampled TMDI maps of Yok Don National Park during the middle of the dry season from 2014 to 2023

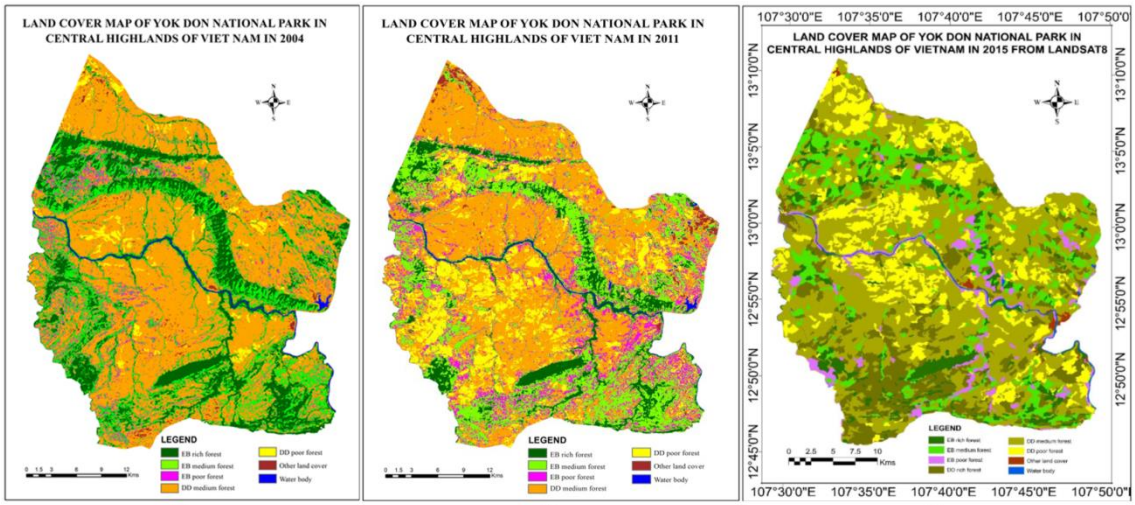

(a) (b) (c)

Figure A-2. Land cover maps of Yok Don National Park for 2004 (a), 2011 (b), and 2015 (c). The land cover maps for 2004 and 2011 were published by Nguyen et al. (2015), while the 2015 map was published by Nguyen et al. (2017)